Crystal Structures of the Binary Ca^{2+} and pdTp Complexes and the Ternary Complex of the $Asp^{21} \rightarrow$ Glu Mutant of Staphylococcal Nuclease. Implications for Catalysis and Ligand Binding†

Andrew M. Libson, Apostolos G. Gittis, and Eaton E. Lattman*

Department of Biophysics & Biophysical Chemistry, The Johns Hopkins School of Medicine, 725 North Wolfe Street, Baltimore, Maryland 21205

Received January 28, 1994; Revised Manuscript Received April 29, 1994®

ABSTRACT: The crystal structure of the $Asp^{21} \rightarrow$ Glu mutant (D21E) of staphylococcal nuclease (SNase) has been determined in three different complex forms. The structure of the D21E ternary complex in which D21E is bound to both Ca^{2+} and the transition-state analogue, thymidine 3′,5′-diphosphate (pdTp), was determined to 1.95-Å resolution. The structures of both binary complexes, D21E bound either to Ca^{2+} or pdTp, were determined to 2.15- and 2.05-Å resolution, respectively. In the ternary structure, we find a 1.5-Å movement of the Ca^{2+} in the active site, evidence of bidentate coordination of Ca^{2+} by Glu^{21} and inner-sphere coordination of the Ca^{2+} by Glu^{43}. Comparison of the D21E binary structures with the ternary model shows large movements of active site side chains expected to play a direct role in catalysis. Glu^{43} moves in the binary nucleotide complex, whereas Arg^{35} is oriented differently in the binary metal complex. From these changes, we seek to explain the basis for the 1500-fold decrease in V_{max} of D21E relative to wild-type SNase (WT). Furthermore, we describe direct structural evidence which explains the cooperativity of Ca^{2+} and pdTp binding in the ternary complex relative to that of the binary complexes.

Staphylococcal nuclease catalyzes the Ca^{2+}-dependent hydrolysis of single- or double-stranded DNA and RNA by cleaving at the 5′ side of a phosphodiester bond, leaving a 3′-phosphonucleotide product (Tucker et al., 1978). The enzyme hydrolyzes polynucleotides at 10^{16} times the rate of unassisted phosphodiester hydrolysis (Serpersu et al., 1987). This dramatic rate enhancement makes SNase a model protein for studying enzyme-catalyzed hydrolysis reactions. The structure of SNase by X-ray crystallography (Cotton et al., 1979; Loll & Lattman, 1989) (see Figure 1), its solution structure by NMR (Torchia et al., 1989; Wang et al., 1990), and NMR docking of the substrate, dTdA (Weber et al., 1992), have been essential in generating structure-based mechanisms for phosphodiester cleavage. In this mechanism, Glu^{43} was proposed to act as a general base activating a nearby water molecule for nucleophilic attack on the phosphodiester phosphorus. Recently, the role of Glu^{43} as a general base has come under intense scrutiny, and there are both kinetic (Poole et al., 1991; Hale et al., 1993) and structural (Judice et al., 1993) studies which have been interpreted to indicate that Glu^{43} may not function as a general base in the hydrolysis reaction. The loss in activity of the Glu^{43} mutants has been proposed to be due to changes in the structure of the adjacent Ω-loop when Glu^{43} is mutated to a residue which cannot function as a general base. The Ω-loop is a flexible, lysine-rich loop near Glu^{43} (residues 45–52). These two studies (Hale et al., 1993; Judice et al., 1993) propose that the Ω-loop's role in hydrolysis is to assist in substrate binding and product release and that Glu^{43} is a structural residue rather than a catalytic one in DNA and RNA hydrolysis.

Arg^{35} and Arg^{87} appear to assist the hydolysis reaction by stabilizing electrostatic interactions and hydrogen bond (H-bond)[1] donation to the charged transition-state intermediate (Serpersu et al., 1987; Judice et al., 1993). It is believed that pdTp represents a transition-state analogue for the SNase reaction (Weber et al., 1993). There is evidence that the transition state of the reaction involves trigonal bipyramidal geometry about the phosphorus and that Arg^{35} and Arg^{87} are each bidentate ligands of this species (Weber et al., 1992). Stereochemical experiments demonstrate that the reaction proceeds with inversion of configuration at phosphorus which further supports the hypothesis that Glu^{43} (which is H-bonded to appropriately positioned water ligands) plays a role in catalysis (Mehdi & Gerlt, 1982). Arg^{87} is considered a possible general acid, protonating the 5′-hydroxyl leaving group. Ca^{2+} is essential for binding both the attacked phosphoryl group and the attacking water and possibly for transition-state stabilization (Weber et al., 1992). SNase is essentially inactive when other multivalent cations are used in the reaction (Tucker et al., 1979).

Kinetic studies of mutants of SNase have been used to test the validity of this model. Mutants of Glu^{43}, Arg^{87}, and Arg^{35} show a dramatic loss in k_{cat} (over 1500-fold less active) (Hibler et al., 1987; Serpersu et al., 1987; Pourmotabbed et al., 1990). These studies have, for the most part, been consistent with the model, but structural studies of some of these mutants have shown that other perturbations away from the mutated side chain may contribute to the reduction in catalysis (Hibler et al., 1987; Pourmotabbed et al., 1990; Loll & Lattman, 1990; Baldisseri et al., 1991).

In this paper, we study by X-ray crystallography the effects of the mutation Asp^{21} to Glu (D21E) on the catalytic and binding properties of SNase. This mutation represents a 1.5-Å lengthening of the side chain of residue 21. Asp^{21} is known

† This work was supported by NIH research grant GM36358. An NSF Biological Centers Award, DIR-8721059, and the W. M. Keck Foundation in part supported this research.

* To whom correspondence should be addressed.

® Abstract published in *Advance ACS Abstracts,* June 1, 1994.

[1] Abbreviations: D21E, $Asp^{21} \rightarrow$ Glu mutant of staphylococcal nuclease; SNase, staphylococcal nuclease; pdTp, thymidine 3′,5′-diphosphate; WT, wild type; H-bond, hydrogen bond; MPD, 2-methyl-2,4-pentanediol; TES, *N*-[tris(hydroxymethyl)methyl]-2-aminoethanesulfonic acid; rmsd, root mean square difference.

0006-2960/94/0433-8007$04.50/0

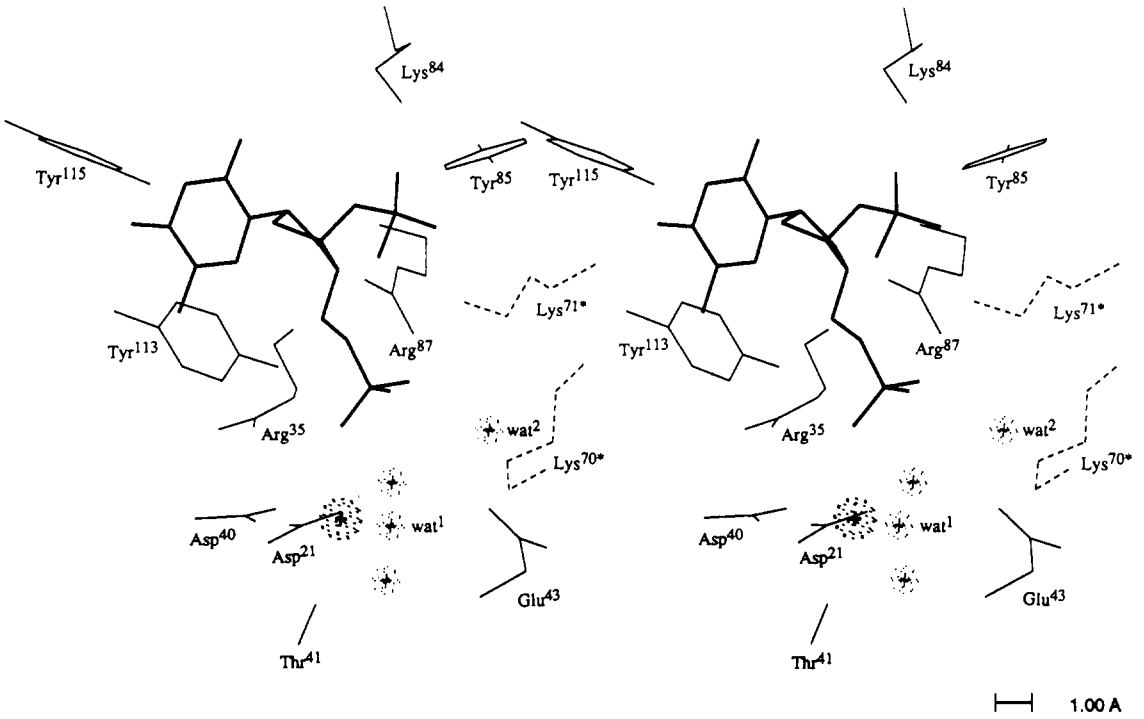

FIGURE 1: Stereo image of the active site of the WT SNase ternary complex. Protein side chains are shown by the light lines and marked accordingly. Thr^{41} binds Ca^{2+} through its carbonyl oxygen. The dashed lines represent side chains from a symmetry-related molecule that make contacts at the active site. The inhibitor, pdTp, is displayed in dark lines. The Ca^{2+} is the large sphere below pdTp. The three inner-sphere water molecules are shown as well as the second-sphere water. Wat^1 is the inner sphere water which is H-bonded to Glu^{43} and is thought to be the attacking nucleophile during polynucleotide hydrolysis. Wat^2 is the second-sphere water which has also been implicated as a possible nucleophile in the hydrolysis reaction. Shown about the pdTp molecule are protein side chains which make van der Waals and H-bond contacts with the inhibitor molecule.

to coordinate Ca^{2+} in the WT structure but is not thought to play a direct role in catalysis. Although D21E binds Ca^{2+}, pdTp, and substrate with the same affinity as WT SNase, D21E shows a 1500-fold decrease in k_{cat} relative to WT (Serpersu et al., 1987). There is also evidence that the conformation of an authentic substrate of SNase, dTdA, is altered in D21E when compared to its structure bound to WT SNase (Weber et al., 1994).

Here, we determine the structure of the [D21E/Ca^{2+}/pdTp] complex (1ENC, Brookhaven Protein Data Base) to rationalize the reduced catalytic rate in D21E. In the structure of the D21E ternary complex, [D21E/Ca^{2+}/pdTp], the Ca^{2+} has moved 1.5 Å away from its position in the WT enzyme. Furthermore, Glu^{43} is an inner sphere ligand directly coordinated to Ca^{2+} in a syn conformation (in which the C–O–Ca^{2+} angle is between 0 and 80°) (Carrell et al., 1988) rather than interacting with Ca^{2+} through a water molecule as a second sphere complex. Also, in the D21E ternary complex the remainder of the solvent structure about the metal ion is severely perturbed. From these studies, we propose that Glu^{43}, while possibly not acting as a general base, is critical for binding a nearby water molecule and positioning it for a nucleophilic attack on the phosphodiester phosphorus. Given the inner sphere coordination of Glu^{43} to Ca^{2+} in D21E, we believe it is unlikely that Glu^{43} is simply playing a structural role in catalysis by altering Ω-loop flexibility and structure.

Binding studies of both the binary metal, [D21E/Ca^{2+}], and the binary nucleotide, [D21E/pdTp], complexes (Serpersu et al., 1987,1988; Weber et al., 1990) show that the binding of pdTp or Ca^{2+} is not as tight in the respective binary complexes as it is in the ternary complex. We have determined the structure of the binding intermediates of D21E, [D21E/pdTp], and [D21E/Ca^{2+}] and use these structures to clarify the cooperative nature of ligand binding in the ternary complex relative to the binary complexes. Also, by examining changes in the active site in proceeding from the binary complexes to the ternary complex, we get a dynamic view of how SNase binds metal and pdTp and how it orients side chains necessary for full catalytic function.

In the binary [D21E/pdTp] complex (2ENB, Brookhaven Protein Data Base), a water molecule replaces Ca^{2+} at the metal binding site, and Glu^{43} points away from the active site. In the binary [D21E/Ca^{2+}] complex (1ENA, Brookhaven Protein Data Base), Glu^{43} displays syn coordination of Ca^{2+}, and Arg^{35} changes its orientation. By comparing these structures with that of the D21E ternary complex, we obtain a structural explanation for the cooperativity of Ca^{2+} and pdTp binding in going from each binary complex to the ternary complex. A preliminary abstract of this work has been published (Libson et al., 1994).

MATERIALS AND METHODS

Protein Purification and Crystal Growth. Isolation of the mutant D21E staphylococcal nuclease from an engineered strain of *Escherichia coli* carrying the expression plasmid pFOG405 and purification to homogeneity was performed as described previously (Shortle & Lin, 1985; Serpersu et al., 1986, 1987). All crystals of D21E were grown by the vapor diffusion technique as described for WT SNase (Loll & Lattman, 1989) at 4 °C using 18 mg/mL of D21E protein solution and various concentrations of 2-methyl-2,4-pentanediol (MPD) as the precipitant. [D21E/Ca^{2+}/pdTp] crystals formed in 50 mM *N*-[tris(hydroxymethyl)methyl]-2-aminoethanesulfonic acid (TES) buffer pH 7.5 containing 10 mM Ca^{2+}, 10 mM pdTp, and 50–52% (v/v) MPD. Crystals of [D21E/pdTp] formed in 50 mM TES buffer pH 7.5 containing 10 mM pdTp and 32–34% (v/v) MPD. Crystals of [D21E/Ca^{2+}] formed in 50 mM tris(hydroxymethyl)-aminomethane (Tris-Cl) buffer pH 8.0 containing 10 mM Ca^{2+} and 65–67% (v/v) MPD. In most cases, large single

Table 1: Collection Statistics and Refinement Parameters on Both Binary Complexes and the Ternary Complex of D21E

	D21E/pdTp	D21E/Ca^{2+}	D21E/Ca^{2+}/pdTp
data collectn statistics			
space group	$P4_1$	$P4_1$	$P4_1$
unit cell (Å)	a = 48.77	a = 47.29	a = 48.05
	b = 48.77	b = 47.29	b = 48.05
	c = 63.44	c = 63.40	c = 63.00
resolution (Å)	6.00–1.95	6.00–2.08	6.00–1.89
N_{obs}	37 566	16 727	44 141
N_{unique}	8297	7583	9811
R_{sym}[a]	4.3	10.7	4.6
completeness (%)	80	89	85
final refinement params			
resolution (Å)	6.00–2.05	6.00–2.15	6.00–1.95
R factor[b]	0.177	0.225	0.174
no. of reflns	7556	7003	9312
no. of atoms	1149	1119	1155
no. of water molecules	38	32	44
rms devn from ideal geometry			
distances (Å)			
bond	0.010	0.010	0.011
angle	0.037	0.035	0.034
chiral center vol (Å^3)	0.116	0.114	0.128
torsion angles (deg)			
planar	3.5	3.2	3.1

[a] $R_{sym} = \sum_h\sum_i I_i(h) - \langle I(h)\rangle|/\sum_h\sum_i I_i(h)$. $I(h)$ is the intensity of reflection h. $\sum_h$ is the sum over all reflections. $\sum_i$ is the sum over the different and symmetry related measurements of a given reflection, $I_i(h)$. [b] R factor $= \sum_h|F_{obs}(h) - F_{calc}(h)|/\sum_h F_{obs}(h)$.

crystals were grown in 1–2 weeks. In the case of [D21E/Ca^{2+}], large single crystals were difficult to isolate, and single crystals appeared sporadically with most conditions giving only a shower of needle-like crystals. All crystals are isomorphous with WT SNase having a $P4_1$ space group. Unit cell dimensions were similar for all crystals. [D21E/Ca^{2+}/pdTp] has $a = b = 48.05$ Å and $c = 63.00$ Å. [D21E/pdTp] has $a = b = 48.77$ Å and $c = 63.44$ Å. [D21E/Ca^{2+}] has $a = b = 47.29$ Å and $c = 63.40$ Å.

Data Collection and Reduction. All data were collected using a Xentronics multiwire area detector mounted on a Huber four-circle goniostat using a Rigaku RU-200 rotating anode X-ray generator equipped with a graphite monochromator. Data frames were processed and reduced with the XENGEN (Howard et al., 1987) software package yielding data collection statistics shown in Table 1. The binary [D21E/Ca^{2+}] statistics have a completeness of 80% for the resolution range of 6.00–2.08 Å. The R_{sym} (on intensity) of 10.7% for the binary metal complex is higher than for the other crystal forms, and the number of observations/reflection is lower than in the two other data sets. This was the best data set obtainable given the difficulty in producing large diffraction-quality crystals of [D21E/Ca^{2+}].

Refinement. The coordinates of WT SNase (Loll & Lattman, 1989) were used as an initial model for the structure determination of the [D21E/Ca^{2+}/pdTp] and [D21E/Ca^{2+}] complexes. To eliminate biases in the initial electron density maps, the starting model contained no pdTp, Ca^{2+}, or solvent molecules and WT Asp^{21} was changed to Gly. The refinement program used was XPLOR, and the simulated annealing protocol was applied (Brunger, 1992). After one cycle of simulated annealing, electron density maps with coefficients $[(2F_o - F_c)\exp(i\alpha_c)]$ and $[(F_o - F_c)\exp(i\alpha_c)]$ were calculated (where F_c and α_c are the amplitude and phase of the structure factor calculated from the model and F_o is the observed structure factor amplitude). The maps were displayed on either an Evans & Sutherland graphics system using the package FRODO (Jones, 1978) or on a Silicon Graphics IRIS workstation using the program CHAIN (Sack, 1988).

In the [D21E/Ca^{2+}/pdTp] initial $2F_o - F_c$ map, well-defined electron density contoured at 1.0σ could be seen for both the pdTp molecule and for the side chain of residue 21. After the pdTp molecule and the Glu side chain were placed into the electron density, a new cycle of simulated annealing was performed and another set of maps was calculated. At this stage, water molecules and the active site Ca^{2+} were identified by looking for both regions of spherical $2F_o - F_c$ density contoured at 1.0σ and $F_o - F_c$ density contoured at 3.5σ. Solvent molecules were placed in the electron density only if they occupied positions with good H-bonding geometry to the protein and were within a 3.0-Å distance of a possible proton donor or acceptor; otherwise, the electron density was ignored. After positions were assigned to all identifiable water molecules in the two maps, several cycles of positional and isotropic B-factor refinement were run on the new model. Using the maps generated after successive cycles of refinement, some minor adjustments in the side chain orientations were manually made and new water molecules were added. After refinement with XPLOR, the geometry of the protein molecule was optimized by running several cycles of stereochemically-restrained least-squares refinement, PROLSQ (Hendrickson, 1985), and a set of new maps was calculated. Where appropriate, alternate conformations of flexible side chains were added, and further refinement with PROLSQ was carried out to give the final model. The [D21E/Ca^{2+}/pdTp] model has a crystallographic R factor of 0.175 for all data between 6.0 and 1.95 Å resolution, with 44 water molecules and individual isotropic temperature factors and water occupancies refined.

The refinement of the two binary complexes, [D21E/Ca^{2+}] and [D21E/pdTp], was carried out in the same way as described above with the following differences. In the case of the [D21E/Ca^{2+}] complex, a 2σ cutoff on the structure factors amplitudes was introduced, while for the [D21E/pdTp] complex, the initial model was that of the D21E ternary complex with solvent molecules, Ca^{2+}, and pdTp removed. The crystallographic parameters at the end of refinement are summarized in Table 1.

Structure Analysis. The final structures were compared after refinement by aligning along the main chain C_α, carbon, and nitrogen atoms using the program XPLOR.

Structure Stereochemistry and Error. All three structures were examined for proper stereochemistry by calculating a Ramachandran plot for the structures. For all the structures, the ϕ and ψ angles conformed to allowed regions of the ϕ,ψ map except for residue Asn^{138}. This residue adopts sterically unfavorable backbone torsion angles due to side chain interactions with the backbone carbonyl of Glu^{106}. Asn^{138} is in electron density in all D21E structures and does not conform to normal backbone geometry in other SNase structures (Loll & Lattman, 1989; Hynes & Fox, 1991).

Luzzati plots were calculated to determine the mean absolute error in atomic position for the three structures (Luzzati, 1952). [D21E/Ca^{2+}/pdTp] had the lowest average positional error of 0.22 Å. [D21E/pdTp] and [D21E/Ca^{2+}] had an average error in atomic position of 0.25 and 0.28 Å, respectively.

RESULTS

Comparison of D21E Ternary Complex and WT Backbones. Comparison of the refined D21E ternary complex aligned with the refined WT ternary complex reveals only a few major changes in the backbone arrangement of D21E. Most of the D21E C_α remain within 0.1–0.3 Å of the WT structure. Major backbone changes occur in three regions of the D21E structure. The first prominent backbone shift is

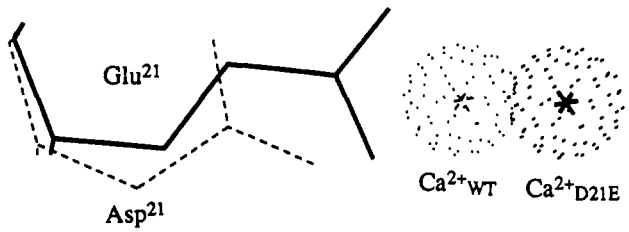

FIGURE 2: Drawing showing movement of Ca^{2+} in response to D21E mutation. Dashed lines represent the structure of the WT residue in the ternary complex. Solid lines show the arrangement of the D21E residue in the ternary complex. $Ca^{2+}{}_{WT}$ is the WT metal. $Ca^{2+}{}_{D21E}$ is the metal in the mutant structure.

seen at residues 40–42 with a C_α–C_α root mean square difference (rmsd) ranging from 0.45–0.6 Å which relaxes to a difference of about 0.35 Å at residues 43 and 44. The next region of major C_α–C_α differences occurs at residues 45–50, along a flexible Ω-loop, which has large C_α backbone differences from 0.5 to 1.5 Å. The final area of significant main chain movement is at the C_α of residues 69–70 which have an rmsd of 0.38 and 0.60 Å, respectively.

Comparison of [D21E/Ca^{2+}] and [D21E/Ca^{2+}/pdTp] Backbones. The rmsd values of 0.1–0.3 Å for the C_α atoms show that the backbone structures of the D21E binary metal and ternary complex are highly superimposable. There are several regions where the C_α rmsd shows larger deviations. The region spanning residues 28–34 has an rmsd slightly higher than average with values ranging from 0.33 to 0.45 Å. From residues 68–84 and 112–117, the C_α backbone is displaced significantly in the binary metal complex in comparison to the ternary backbone with C_α rmsd's of 0.33–0.64 Å and 0.39–0.62 Å, respectively. These two backbone regions have side chains primarily responsible for binding the pdTp nucleotide in both the D21E and WT ternary complexes (see Figure 1). The Ω-loop shows the greatest deviation with a C_α rmsd of 0.45–2.21 Å from residues 43–51.

Comparison of Binary [D21E/pdTp] and Ternary [D21E/Ca^{2+}/pdTp] Backbone Structures. The C_α rmsd are similar in the two structures with C_α–C_α differences of only 0.1–0.3 Å in most regions. There are two regions of the structure where differences greater than the average occur. Again, the Ω-loop between residues 43 and 52 shows a C_α rmsd ranging from 0.43 to 2.00 Å. In a smaller region, at residues 84–86, C_α differences of 0.38–0.43 Å appear.

Comparison of the Active-Site Regions of D21E and WT Ternary Complexes. There are several significant differences in the active-site arrangement of the D21E complex in comparison with that of the WT complex. First, the D21E Ca^{2+} moves 1.5 Å away from the negatively charged pocket in which it rests toward exposure into bulk solvent (Figure 2). This shift of Ca^{2+} in D21E corresponds to the 1.5-Å increase in the length of residue 21 when a methylene group is added to make the Asp^{21} to Glu^{21} mutation. The mutated Glu^{21} residue literally pushes the Ca^{2+} out of the active site by 1.5 Å. The Ca^{2+} movement is in the direction of Glu^{43} and Asp^{40} as they are positioned in the WT structure. Residue 21 changes from a monodentate (Asp) to a bidentate (Glu) ligand.

The Ca^{2+} movement has dramatic effects on metal coordination at the active site (see Figure 3B). In the D21E ternary complex, Glu^{43} (which binds Ca^{2+} indirectly through a coordinating water in the WT complex (through H_2O^1 in Figure 3A)) displays syn coordination of Ca^{2+} at an inner sphere position previously occupied by a water (H_2O^3 is replaced by Glu^{43}). There is electron density for positioning of the Glu^{43} side chain in the D21E ternary complex (see Figure 4). The water replaced by Glu^{43} in the D21E ternary structure is *cis* to the Glu^{21} ligand. In the WT structure (see Figure 3A), there is a water molecule (H_2O^1) bridging the metal ion and Glu^{43}. This water, which is *trans* to Glu^{21}, is not seen in the D21E complex despite the space available on Ca^{2+} for water coordination at that site. Neither $2F_o - F_c$ nor $F_o - F_c$ density is observed at this site suggesting, at best, that a transiently bound water molecule exists at the position *trans* to Glu^{21}. In the WT structure, this water is the most likely candidate as the attacking nucleophile which displaces the 5′ oxygen of the nucleotide during SNase hydrolysis (Weber et al., 1992). Because the Glu^{43} side chain moves in order to coordinate Ca^{2+} in D21E, there is no second sphere water in the D21E ternary structure.

In D21E, Glu^{21} displays bidentate chelation of the Ca^{2+}. This is described by Carrell (Carrell et al., 1988) as "direct" coordination in which the C–O–Ca^{2+} angle is between 80 and 90° and both carboxylate oxygens are equidistant from the bound metal. Asp^{21} is a monodentate ligand of Ca^{2+} in the WT structure. Both D21E and WT Ca^{2+} share heptacoordinate geometry. In the WT structure, the carbonyl oxygen of Thr^{41} and a coordinating water (H_2O^2 from Figure 3A) occupy the shared axial position opposite the other axial ligand, the oxygen of the 5′ phosphate of the pdTp inhibitor. In D21E, it is the bidentate coordination of Glu^{21} which occupies the shared axial position. The other axial ligand is not identified in the structure but is presumed to be the transiently bound water possibly involved in polynucleotide hydrolysis (see Figure 5). In D21E, the carbonyl oxygen of Thr^{41} occupies an equatorial coordination site exactly 180° across the metal ion from the oxygen of the 5′ phosphate of pdTp. This angle in the WT structure is 150° which allows a coordinated water to share the axial position with the Thr^{41} carbonyl oxygen (see Figure 5). In D21E, where the carbonyl oxygen of Thr^{41} is 180° from the opposite ligand, Thr^{41} cannot share the axial ligand position if Ca^{2+} is to maintain a heptacoordinate geometry. In WT, the equatorial sites are occupied by the β-carboxylate oxygens of Asp^{21} and Asp^{40} and two coordinating waters. In D21E, the equatorial ligands are the oxygen of the 5′ phosphate of pdTp, the carbonyl oxygen of Thr^{41}, a γ-carboxylate oxygen of Glu^{43}, and a β-carboxylate oxygen of Asp^{40}. The inhibitor, pdTp, displays similar geometry and positioning in both D21E and WT complexes. The only notable difference is a slight twist of the oxygens about the 5′ phosphate which amounts to a rotation of approximately 10–15° about the O5′–P5′ bond.

Arg^{87} and Arg^{35} of both D21E and WT complexes orient identically relative to the 5′ phosphate of pdTp. Arg^{35} makes bidentate H-bonds to the inhibitor. The hydrogen of the η-nitrogen H-bonds to the 5′ phosphate oxygen bound to Ca^{2+}. The hydrogen of the ε-nitrogen H-bonds to a noncoordinated oxygen. Arg^{87} also makes bidentate H-bonding to the oxygens of the 5′ phosphate of pdTp. Hydrogens from both the η-nitrogens of Arg^{87} are H-bonded to pdTp. One amine group H-bonds to a noncoordinated oxygen while the other H-bonds to the oxygen which is bound to the 5′ carbon of the nucleotide sugar. This oxygen would be the leaving oxygen of a substrate.

Differences in Crystal Packing between D21E and WT Ternary Complexes. In all ternary WT and mutant structures, Lys^{70} and Lys^{71} make salt bridges with atoms in the active site of symmetry related molecules (see Figure 1). The ε-amine group of Lys^{71} in both D21E and WT lies between the two negatively charged phosphate groups of the pdTp in a symmetry-related molecule. Lys^{71} H-bonds with both the 3′ and the 5′ phosphates and displaces the 3′ phosphate farther from the 5′ phosphate than found in the NMR solution structure of pdTp in the WT/Ca^{2+}/pdTp structure (Weber et al., 1993). Presumably, the solution structure of enzyme-

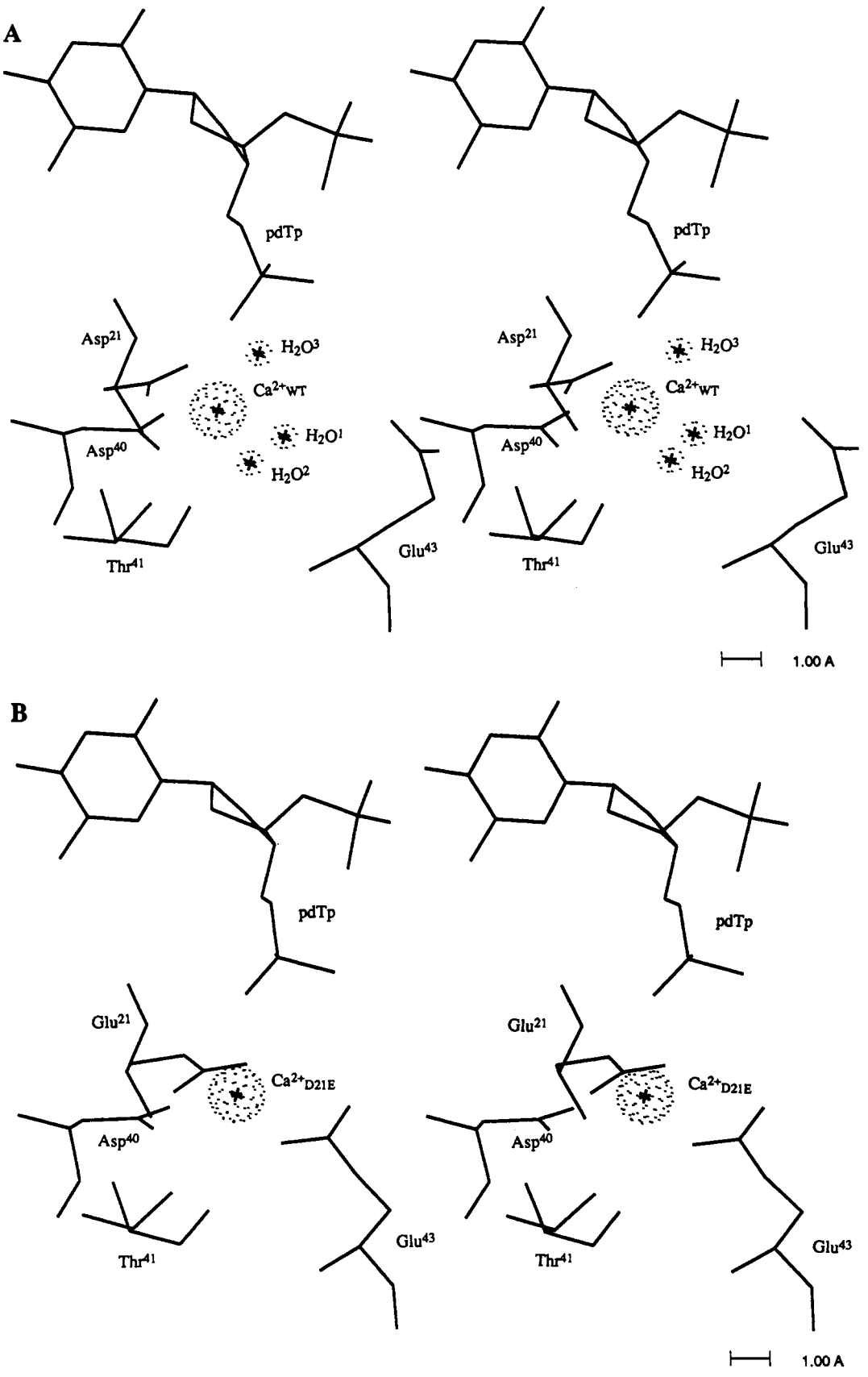

FIGURE 3: Stereo diagram of the active sites of the WT and D21E ternary complex. (A) Active site of the WT ternary complex. Included are the three water molecules coordinated to Ca^{2+}. H_2O^1 is the water molecule which binds to Glu^{43} and most likely the attacking nucleophile of the phosphodiester phosphorus. H_2O^2 and H_2O^3 are noncatalytic water molecules which complete the coordination of heptacoordinate Ca^{2+}. (B) Active site of D21E ternary complex. Note absence of any crystallographic water molecules and addition of protein ligand, Glu^{43}, which lies *cis* to the coordinating oxygens of Glu^{21}. *Trans* of Glu^{21} lies a space available for binding a water molecule. In both cases, Thr^{41} coordinates Ca^{2+} through its carbonyl oxygen.

bound pdTp is more representative of the real geometry of the inhibitor when bound to SNase since it is not perturbed by Lys^{70} and Lys^{71} crystal contacts. Lys^{70} of D21E is oriented near a noncoordinated oxygen of the 5' phosphate of pdTp and the γ-carboxylate of Glu^{21}. Lys^{70} is well within 3 Å of both Glu^{21} and pdTp. Conversely, WT Lys^{70} makes a salt

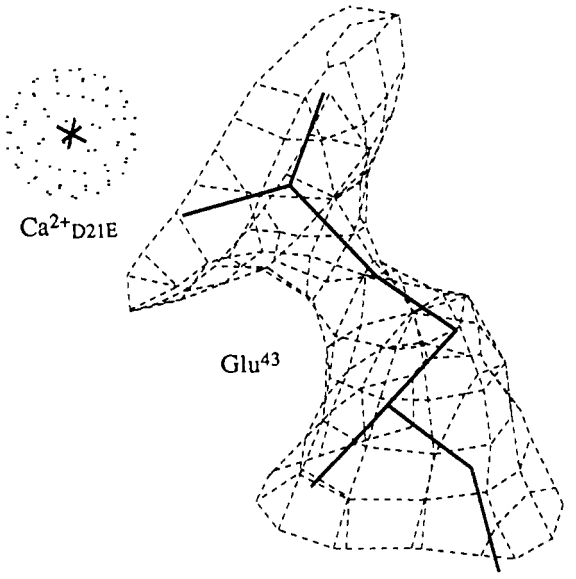

FIGURE 4: Difference density about Glu^{43} in D21E ternary complex. An $F_o - F_c$ omit map was calculated and contoured at 2σ. Within the density is a trace of the Glu^{43} side chain from the refined model of the D21E ternary complex.

bridge with Glu^{43} which lies within 3 Å of the lysine amine.

Comparison of [D21E/Ca^{2+}] Binary Complex and D21E Ternary Complex at the Active Sites. The binary metal complex and the ternary complex of D21E share nearly identical coordination. The Ca^{2+} of the binary complex has no ligand in the position taken by pdTp in the ternary complex. In the binary metal complex, there is no identifiable water coordinated to Ca^{2+} at the site occupied by the 5′ phosphate oxygen of pdTp in the ternary complex. There is a possible second-sphere water 5.5 Å away from Ca^{2+} near the site normally occupied by the 5′ phosphorus of pdTp (see Figure 6). Both structures display heptacoordinate geometry. In both complexes, Glu^{21} is a bidentate ligand of Ca^{2+}. Also, Ca^{2+} is syn coordinated by Glu^{43} in both structures. In [D21E/Ca^{2+}], the γ-carboxylate of Glu^{43} is 0.6 Å farther from Ca^{2+} than in the ternary D21E complex (see Table 2). There are no waters identified as coordinating Ca^{2+} in either the D21E binary metal or ternary complexes. The Ca^{2+} ions are not superimposable in the aligned structures. The binary metal Ca^{+2} lies 0.5 Å away from the ternary Ca^{2+} (see Figure 6). This movement brings it exactly 0.5 Å closer to the carbonyl oxygen of Thr^{41} in the binary metal complex and 0.5 Å farther from where the 5′ phosphate ligand of pdTp would bind in the ternary complex (see Table 2).

Arg^{87} is superimposable in both structures. Arg^{35} is perturbed significantly in the binary metal complex (see Figure 7). The η-nitrogen of the Arg^{35} amine normally H-bonded to pdTp is in the same position, but the Arg^{35} side chain in the D21E binary metal complex has been twisted so that the other η-nitrogen of the Arg^{35} amine is 90° from where the corresponding, noninteracting η-nitrogen is located in the ternary D21E complex. The ε-nitrogen is pointed toward the 5′ phosphate oxygen of the inhibitor in the ternary complex and lies well within H-bonding distance (2.92 Å). The ε-nitrogen of the binary metal complex is pointed away from the position occupied by the inhibitor in the ternary complex and is 4.06 Å away from the site of the 5′ phosphate oxygen.

Changes in Nucleotide Binding Residues in the [D21E/Ca^{2+}] Binary Complex. Side chains responsible for binding the pdTp molecule are shown in Figure 1. Changes in the arrangement of nucleotide binding side chains are noted by comparing the binary metal and the ternary D21E complexes. Tyr^{113} and Tyr^{115}, which are within van der Waals contact distance of the nucleotide in the ternary complex, have different conformations in the binary metal complex. In [D21E/Ca^{2+}], these side chains are shifted out into bulk solvent away from the position occupied by the nucleotide. Also, Tyr^{85} has also moved away from the region where pdTp resides, although not as dramatically as Tyr^{113} and Tyr^{115}. Lys^{84} forms a salt bridge with the 3′ phosphate of the inhibitor in the D21E ternary complex. In the binary metal complex, Lys^{84} is pointed away from pdTp site directly into solvent.

Crystal Contacts in the [D21E/Ca^{2+}] Complex. Lys^{70} makes a hydrogen bond with Glu^{21} from a symmetry-related molecule in the D21E binary complex just as it does in the D21E ternary complex. Lys^{71}, which extends in between the 3′ and 5′ phosphate of a symmetry-related pdTp molecule in the ternary complex, is found in a bent conformation in the binary complex. Lys^{71} does not interact with any symmetry-related molecules in the binary metal complex since pdTp is not available to orient the Lys side chain. Instead, Lys^{71} is exposed to bulk solvent in the binary metal complex.

Comparison of [D21E/pdTp] and [D21E/Ca^{2+}/pdTp] Active Site Structures. As shown in Figure 8, the site occupied by Ca^{2+} in the ternary D21E complex is occupied by a water molecule in the binary nucleotide complex. This water molecule is within H-bonding distance of the β-carboxylate oxygen of Asp^{40} (2.44 Å) and the γ-carboxylate oxygen of Glu^{21} (2.48 Å) (from Table 2). Recall that Glu^{21} in the binary metal and ternary complex binds the metal as a bidentate ligand with both γ-carboxylate oxygens equidistant from the metal (approximately 2.7 Å). In the binary nucleotide complex,

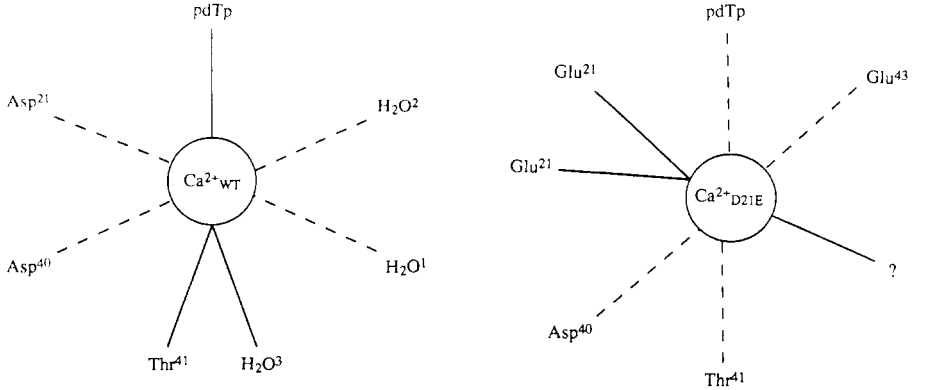

FIGURE 5: Coordination geometry about Ca^{2+} in WT and D21E SNase. The WT Ca^{2+} coordination is shown on the left. The mutant D21E structure is shown on the right. In both heptacoordinate structures, the dashed lines represent equatorial ligands and the solid lines represent axial ligands. Glu^{21} is shown bound at two positions in the D21E structure since it chelates Ca^{2+} with both carboxylate oxygens of the side chain. The other axial position in the D21E structure is represented by a ? since no ligand was identified at that position in the crystal structure. It is presumed that a transiently bound water molecule occupies this site.

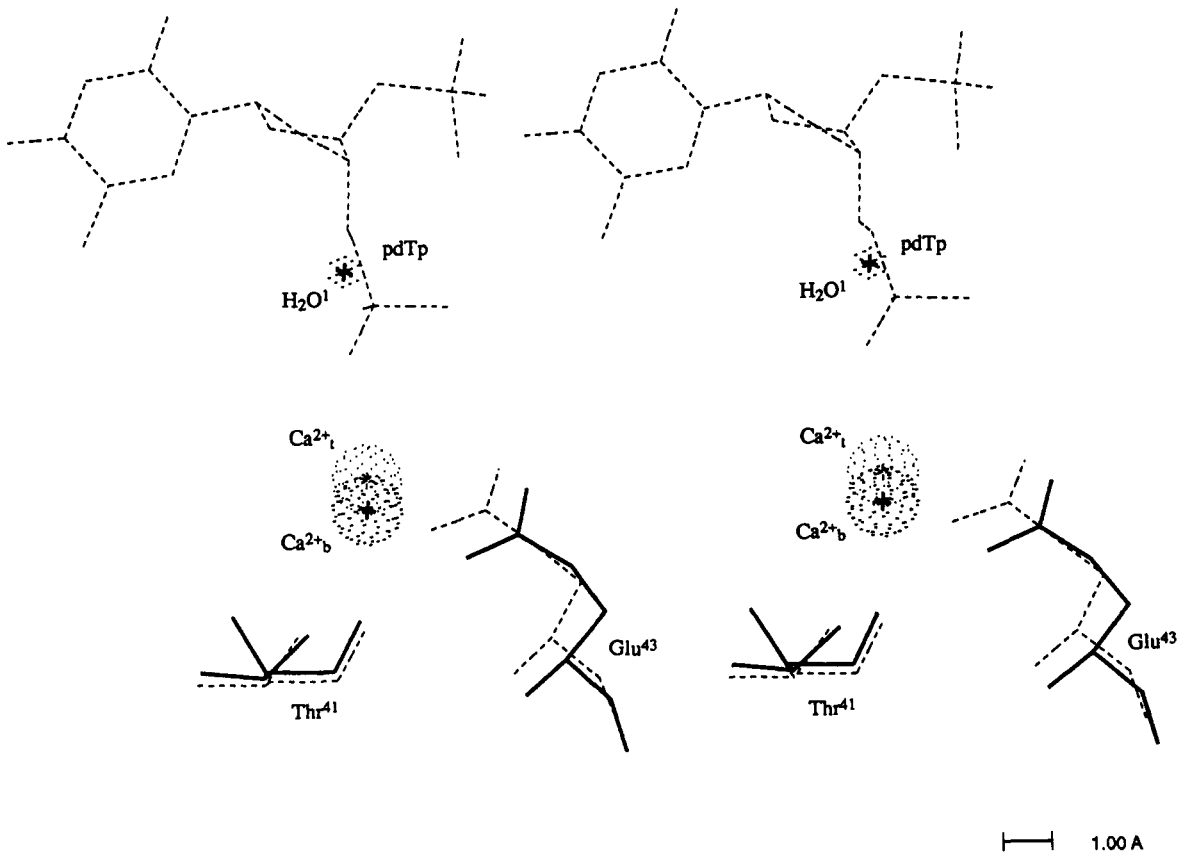

FIGURE 6: Stereo image of the superposition of active sites of [D21E/Ca^{2+}/pdTp] and [D21E/Ca^{2+}]. The dashed lines show the arrangement of atoms in the ternary complex. The solid lines show the arrangement of atoms in the binary metal complex. Ca^{2+}_t is the metal for the ternary complex, while Ca^{2+}_b is the metal for the binary complex. H_2O^1 is a water molecule which shows up in the binary metal complex when pdTp is not present.

Table 2: Distances from Closest Coordinating Atom of Active Site Residue to either Ca^{2+} or H_2O

residue	D21E/Ca^{2+}	D21E/pdTp[a]	D21E/Ca^{2+}/pdTp	WT
Glu^{21}	2.65 & 2.75	2.48 & 2.67	2.69 & 2.66	
Asp^{21}				2.39
Asp^{40}	2.37	2.44	2.16	2.31
Thr^{41} (C=O)[c]	2.40	3.44	3.25	2.67
Glu^{43}	2.55	5.10	1.91	4.70
pdTp (P–O)[d]	5.56[b]	3.05	2.73	2.74

[a] Distances are from residues to water molecule which occupies Ca^{2+} position in the structure. [b] Distance from Ca^{2+} to water molecule located where pdTp is normally found. [c] Represents distance from mainchain carbonyl O to metal center. [d] Represents distance from closest 5′ phosphate O to metal center.

Glu^{21} is in a syn conformation relative to the active site water molecule, with one γ-carboxylate oxygen farther away (2.68 Å) from the solvent molecule than the other (2.48 Å). The oxygen of the 5′ phosphate, which is within coordinating distance of the Ca^{2+} in the ternary complex (2.73 Å), is shifted from the active site water molecule in the binary nucleotide complex (3.04 Å). Indeed, the entire pdTp molecule in the binary complex is shifted away from the active site by about 0.40–0.45 Å relative to the pdTp position in the ternary complex. Also, in [D21E/pdTp], Glu^{43} does not orient into the active site (presumably due to the absence of the metal ion to coordinate) but has its side chains pointing out toward the Ω-loop where it is within H-bond distance of the main chain amide hydrogens of residue 44 and 45 (2.7–2.8 Å) and within 2.49 Å of the hydroxyl group of Thr^{44}. The nearest γ-carboxylate of Glu^{43} is over 5 Å away from the active site water molecule (see Figure 8). In the ternary complex, Glu^{43} is 2 Å away from the Ca^{2+} center.

DISCUSSION

Comparison of Backbone Structures. Both the ternary and the two binary complexes of D21E show large differences in their main chain structure at the Ω-loop between residues 44 and 52. The Ω-loop differences are primarily attributed to the poor density in these regions due to the increased flexibility of this loop. The NMR structure of WT SNase shows extreme flexibility in this Ω-loop region suggesting that no single conformation exists for this loop (Torchia et al., 1989). Other backbone movements can be explained as direct results of the D21E mutation. In the comparison of ternary D21E and WT complexes, the shift of D21E residues 40–42 is attributed to the movement of Asp^{40} as it shifts in response to the movement of Ca^{2+} out of the active site pocket. The 1.5-Å displacement of Ca^{2+} causes the side chain of Asp^{40} to shift approximately 0.7 Å and the main chain to move 0.4 Å as Asp^{40} attempts to maintain proper coordination geometry with the metal ion. The large C_α rmsd at Lys^{70} is due to changes in crystal packing. Lys^{70} in the D21E ternary complex reaches deeper into the active site of a symmetry-related molecule and H-bonds with Glu^{21} and the 5′ phosphate of pdTp. This perturbs the loop in which Lys^{70} is found, thus reinforcing the idea that loop structures of proteins determined by X-ray crystallography are often extremely sensitive to crystal packing forces.

The backbone movement of residues 28–34 in the binary metal [D21E/Ca^{2+}] complex relative to the ternary D21E structure cannot be explained readily but may be a result of the movement of Arg^{35} in the binary metal structure. The large C_α rmsd in residues 68–84 and 112–117 are most likely due to the lack of pdTp in the structure since side chains in this region are responsible for binding the nucleotide through either charge interactions, H-bonds, or van der Waals contacts. The backbone of the binary metal complex is more open in

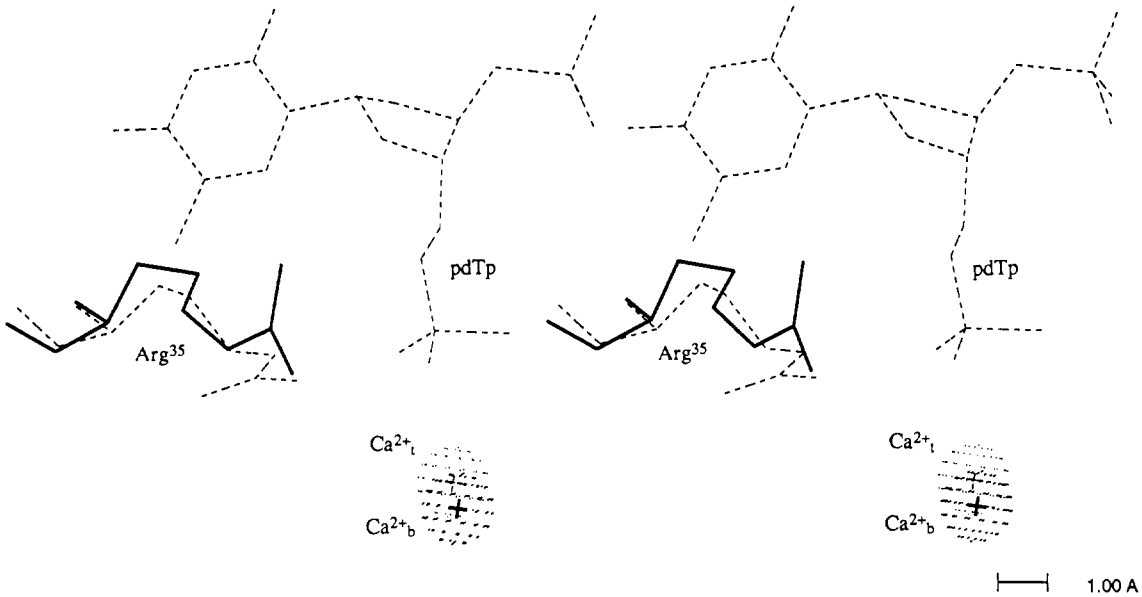

FIGURE 7: Stereo image comparing the Arg^{35} orientation in [D21E/Ca^{2+}/pdTp] and [D21E/Ca^{2+}]. Ternary complex residues are shown by the dashed lines. The binary metal complex residues are shown by the solid lines. Ca^{2+}_t is the metal for the ternary complex, while Ca^{2+}_b is the metal for the binary complex.

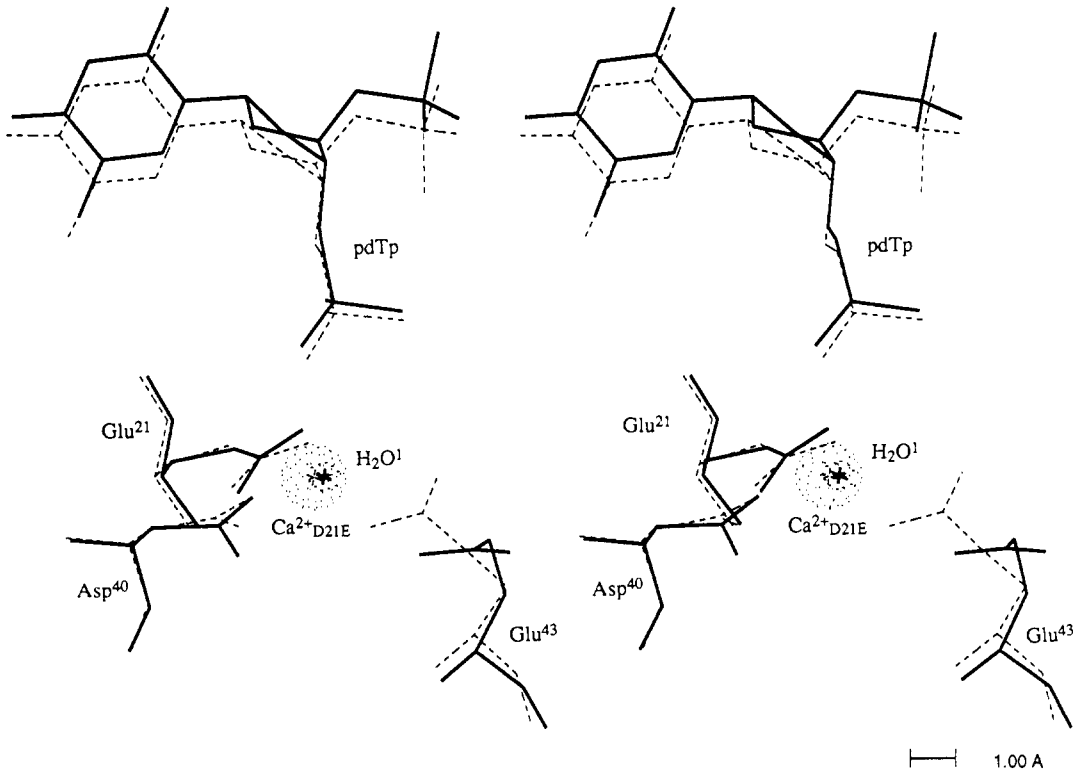

FIGURE 8: Stereo image of the superposition of active sites of [D21E/Ca^{2+}/pdTp] and [D21E/pdTp]. The dashed lines represent arrangement of atoms in the ternary complex. The solid lines show arrangement of atoms in binary nucleotide structure. The metal center (Ca^{2+}_{D21E}) of the ternary complex and the water molecule (H_2O^1) which occupies that site in [D21E/pdTp] are almost identical.

this region, and it appears that SNase makes significant changes in its backbone arrangement in order to bind nucleotide. It may be presumed that similar shifts will be seen with an authentic polynucleotide substrate.

The main chain perturbation seen in the binary nucleotide structure [D21E/pdTp], in comparison with the D21E ternary complex, can be explained as a movement in response to the 0.4 Å shift in the entire pdTp molecule. In the binary nucleotide complex, pdTp is 0.4 Å farther from the position of active site Ca^{2+} than in the ternary D21E complex. The backbone moves to compensate for this shift indicating that the loop from residue 78–87 acts as a clamp to bind the nucleotide. Furthermore, it offers a structural explanation for the fact that binding of nucleotide in the binary complex is much weaker than in the ternary complex (Serpersu et al., 1986, 1987, 1988). There are two main reasons for tighter pdTp binding in the ternary complex. First, the positively charged Ca^{2+} draws the negatively charged 5′ phosphate of the pdTp molecule into the active site by a distance of 0.4 Å and binds the pdTp molecule directly. Second, the protein molecule clamps down on the inhibitor molecule making the ternary complex a more compact, more stable structure by increasing its van der Waals contact surface area with the nucleotide.

It has also been shown that pdTp tightens the binding of Ca^{2+} to SNase. In D21E, the K_d of Ca^{2+} in the binary [D21E/

Ca^{2+}] complex is 19 times higher than the K_d of Ca^{2+} in the ternary [D21E/Ca^{2+}/pdTp] complex (Serpersu et al., 1987). In the binary metal complex, Ca^{2+} shifts by about 0.5 Å in response to the binding of inhibitor just as the inhibitor in the binary nucleotide complex moves when it binds Ca^{2+}. Most likely, a transiently bound water ligand of the metal is replaced by a stably liganded 5′ phosphate when the [D21E/Ca^{+2}] complex is converted to the ternary complex. The negative charge of the pdTp 5′ phosphate attracts Ca^{2+} out of the pocket in forming the ternary complex. A superposition of the two binary structures reveals less compactness and weaker coordination than in the ternary complex. The backbone near pdTp undergoes a 0.4-Å movement, and Ca^{2+} and pdTp are up to 0.9–1.0 Å closer in the ternary structure than in the superimposed binary structures. We conclude that the movements of Ca^{2+}, pdTp, and the protein loops that occur during formation of the ternary complex are direct structural evidence of the cooperativity of protein, metal, and ligand binding. This is of mechanistic significance since pdTp is a transition-state analogue (Weber et al., 1993).

Comparison of Active Sites. D21E is 1500-fold less active catalytically than WT SNase (Serpersu et al, 1988). One would like to be able to compare the active sites of the ternary complexes of WT and D21E and use structural evidence to explain this large loss in activity. While the 1.5-Å movement of the Ca^{2+} in the ternary complex of D21E is dramatic and has profound effects on the coordination of Ca^{2+} in the active site, it is difficult to use the movement of Ca^{2+} alone to explain the loss of activity. The Ca^{2+} movement causes no gross changes in metal to 5′ phosphate distance nor does it dramatically change the position of the inhibitor. Instead, the loss in activity can be explained as a result of the direct coordination of Glu^{43} to Ca^{2+} in the D21E structure. Glu^{43} is no longer available to assist in the stable coordination of a water molecule to Ca^{2+}, and its γ-carboxylate group is too near the 5′ phosphate of pdTp to accommodate a second sphere water between them. It is believed that the inner sphere rather than the second sphere water molecule is the most likely candidate as the attacking nucleophile in the SNase reaction (Weber et al., 1992). Still, neither a second sphere water nor a catalytic inner sphere water are identified in the D21E ternary complex suggesting that if a water is coordinated to Ca^{2+}, it is only transiently bound. Perhaps, this transiently bound water would be a less effective nucleophile than the stably bound water found in the WT structure. The role of Glu^{43} may be to assist Ca^{2+} in stably binding a water molecule facilitating catalysis by approximation and by properly orienting the water or hydroxyl ion for attack. Thus, the D21E mutant, in that it binds Glu^{43} directly to Ca^{2+}, would act much like any Glu^{43} mutation such as E43D and E43Q which are all incapable of properly H-bonding a water when coordinated to Ca^{2+} (Loll & Lattman, 1990). These mutants all show approximately 1500–4000-fold loss (Hibler et al., 1987) in V_{max}/K_m which is the suggested contribution to catalysis that a stably coordinated water near the polynucleotide binding site would offer (Serpersu et al., 1987).

For some time, Glu^{43} was thought to have acted as a general base by removing a proton from either a second-sphere or H-bonded inner-sphere water. This model has been called into question by kinetic studies of WT SNase and a mutant, E43D (Hale et al., 1993), as well as recent structural and kinetic studies of a mutant of SNase in which Glu^{43} was replaced with an unnatural amino acid (Judice et al., 1993). These two studies suggest that Glu^{43} is not acting as a general base and propose that the loss in catalytic activity in Glu^{43} mutants is primarily due to perturbation of the Ω-loop. Hale et al. (1993) and Judice et al. (1993) propose that the primary role of Glu^{43} is as a structural residue binding Ca^{2+} through a water, thereby stabilizing the backbone of residue 43 and adjacent residues including the Ω-loop structure which is suggested to be required for substrate binding and product release. The D21E ternary structure does not support this hypothesis. Glu^{43} remains bound (although not through a water) to Ca^{2+}, and one still sees a loss in hydrolytic activity. Also, while we do see good main chain density for residues 41–44, residues 45–51, which make up most of the Ω-loop, are still in extremely poor density despite the stabilization of Glu^{43}. Thus, the flexibility of the Ω-loop seems entirely insensitive to the tethering of Glu^{43} to the active site Ca^{2+}. Other work has shown that a Ω-loop deletion results in only a 40-fold decrease in V_{max} (Poole et al., 1991). Structural studies of a Δ44–49 deletion of SNase show that the loop is now fixed as a tight β turn (Baldisseri et al., 1991). Mutants of Δ44–49, where the structure of the β turn is preserved, maintain up to 30% WT activity suggesting that the Ω-loop is not essential in SNase catalysis of polynucleotide hydrolysis. Also, the crystal structure of one of these highly active mutants shows Glu^{43} to be indirectly bound to Ca^{2+} through an inner sphere water molecule as it is in WT SNase (S. M. Green, personal communication).

The γ-carboxylate of Glu^{43} is 0.5 Å closer to Ca^{2+} in the D21E ternary complex than in the binary [D21E/Ca^{2+}] complex. Movement of Glu^{43} closer to the metal ion is not understood. It may be that Glu^{43} cannot coordinate the Ca^{2+} as well when it sits deeper in the active site pocket as it does in [D21E/Ca^{2+}]. Metal cations are most often found in the plane of the carboxylate group, and perhaps the ternary complex provides more stable carboxylate binding (Glusker et al., 1991). Ca^{2+} (a hard metal ion held to ligands primarily through electrostatic forces as opposed to covalent bonds) would not make rigid geometrical demands on its ligands, so another explanation may be necessary. The electron density of a $2F_o - F_c$ omit map contoured at 1σ for Glu^{43} is broken between the C_γ and the C_δ in the ternary complex suggesting some flexibility at the carboxylate end of the side chain. While it is clear in both maps that Glu^{43} coordinates Ca^{2+}, the precise position of the γ-carboxylate may be less accurate in the D21E ternary complex than it is in the binary metal complex.

The ternary structure shown here is in agreement with EPR studies of Mn^{2+} coordination in D21E (Serpersu et al., 1988). These studies show that Mn^{2+} in D21E has one less water ligand or, consequently, one more side chain ligand than WT SNase. Mn^{2+} prefers hexacoordinate octahedral geometry and is not likely to be heptacoordinated like Ca^{2+}, so these studies represent a comparison of water coordination at a hexacoordinate Mn^{2+} of D21E and WT SNase. While there is no evidence that Mn^{2+} will bind carboxylate groups of small molecules with bidentate coordination such that both oxygens are equidistant to and contribute equally to metal ion binding (Carrell et al., 1988), in glutamine synthetase approximate bidentate coordination of Mn^{2+} by Glu^{220} has been found (Yamashita et al., 1989). Ca^{2+} shows several examples of bidentate coordination by carboxylate groups (Carrell et al., 1988). It is presumed that Glu^{21} would display monodentate binding of Mn^{2+}. The structural studies reported here support the EPR results and suggest that Glu^{43} is the extra side chain ligand found in D21E but not in WT SNase.

It was suggested earlier that the position of the axial and equatorial ligands of Ca^{2+} are significantly altered in D21E relative to the WT ternary structure. In WT SNase, the carbonyl oxygen of Thr^{41}, a water, and a 5′ phosphate oxygen of pdTp occupy the axial positions. In D21E, the carboxylate

oxygens of Glu^{21} are equidistant from Ca^{2+} (2.65 Å) chelating the metal ion through bidentate coordination. Also, in D21E, the carbonyl oxygen of Thr^{41} is now 180° from the 5′ phosphate oxygen of pdTp making it extremely unlikely that the backbone oxygen of Thr^{41} could occupy one of the two axial positions of a heptacoordinate Ca^{2+}. Instead, if one assumes that Ca^{2+} is still heptacoordinate in D21E, then the most likely axial ligands of D21E Ca^{2+} are Glu^{21} and a water molecule. The water molecule is not seen in the X-ray structure, but an open coordination site does exist for a water ligand, and one might interpret the lack of electron density as evidence of a weakly bound water at that position. While it is possible that no ligand occupies the other axial site, a water ligand is detected by water relaxation and by pulsed EPR in the ternary [D21E/Mn^{2+}/pdTp] complex (Serpersu et al., 1987, 1988). If Glu^{21} can be thought of as an axial, bidentate ligand, similar to carboxylate coordination of all EF hand proteins and many other Ca^{2+} binding proteins (Glusker, 1991), then the 5′ phosphate now occupies an equatorial site on the Ca^{2+}. It is possible this change in coordination *trans* to the substrates might have an effect on SNase hydrolysis.

The active site arrangements of both binary structures provide a unique opportunity to look at changes which occur in the active site upon formation of the ternary complex. The presumption is that significant changes would be seen at residues which play a role in maintaining full catalytic function. In this regard, two main observation may be made from the study of the binary complex active sites. In the binary nucleotide structure, Glu^{43} is pointed away from the active site. We suspect that Glu^{43} is moved by electrostatic repulsion from the negatively charged (2-) 5′ phosphate of pdTp. In the SNase apoenzyme, which has neither pdTp nor Ca^{2+}, the closest γ-carboxylate oxygen is 2.5 Å from the D21E Ca^{2+} center (Hynes & Fox, 1991). Upon metal binding (which forms the D21E ternary complex), Glu^{43} moves directly into the active site by coordinating the metal. Thus, one major consequence of binding Ca^{2+} is the sequestering of Glu^{43} into the active site. In D21E, Glu^{43} binds directly to Ca^{2+} and cannot fulfill its proposed role as H-bonding to a nucleophilic water. It is possible that Ca^{2+} acts similarly in WT SNase. In the binary [D21E/pdTp] complex, Glu^{43} is repelled by the negative charge of the nucleotide inhibitor. In the ternary complex of WT, the positively charged Ca^{2+} draws Glu^{43} closer to the active site where it can accept a hydrogen from a water ligand of the metal ion, stabilizing the coordination of the water molecule.

In the binary metal structure, the primary difference is movement of Arg^{35}. It has been proposed that Arg^{35} binds the substrate as a monodentate H-bond donor (Weber et al., 1992). The bidentate coordination shown in crystal structures of SNase/Ca^{2+}/pdTp represents Arg^{35} binding a transition state, where pdTp represents a transition state analogue. It is believed that the hydrolysis of polynucleotides occurs through a trigonal bipyramidal transition state (Weber et al., 1992). Presumably, Arg^{35}, as well as Arg^{87}, stabilize this transition state via bidentate H-bonding. Arg^{35}, in the binary metal complex of D21E, is clearly oriented to only bind as a monodentate ligand. Upon binding of pdTp, Arg^{35} shifts to its normal bidentate coordination. These two structures offer the first structural support that Arg^{35} can accommodate such a change from a monodentate orientation to a bidentate one.

ACKNOWLEDGMENT

We thank Al Mildvan and David Weber for invaluable discussion and insight. We thank Enrique De La Cruz for proofreading the manuscript.

REFERENCES

Baldisseri, D. M., Torchia, D. M., Poole, L. B., & Gerlt, J. A (1991) *Biochemistry 30*, 3628.
Brunger, A. T. (1992) *XPLOR Manual*, version 3.1, Yale University Press, New Haven, CT.
Carrell, C. J., Carrell, H. L., Erlebacher, J., & Glusker, J. P. (1988) *J. Am. Chem. Soc. 110*, 8651.
Cotton, F. A., Hazen, E. E., & Legg, J. J. (1979) *Proc. Natl. Acad. Sci. U.S.A. 76*, 2551.
Glusker, J. P. (1991) *Adv. Protein Chem. 42*, 3.
Hale, S. P., Poole, L. B., & Gerlt, J. A. (1993) *Biochemistry 32*, 7479.
Hendrickson, W. A. (1985) *Methods Enzymol. 115*, 252.
Hibler, D. W., Stolowich, N. J., Reynolds, M. A., Gerlt, J. A., Wilde, J. A., & Bolton, P. H. (1987) *Biochemistry 26*, 6278.
Howard, A. J., Gilliland, G. L., Finzel, B. C., Poulos, T. L., Ohlendorf, D. H., & Salemme, F. R. (1987) *J. Appl. Crystallogr. 20*, 383.
Hynes, T. R., & Fox, R. O. (1991) *Proteins 10*, 92.
Jones, T. A. (1978) *J. Appl. Crystallogr. 11*, 268.
Judice, J. K., Gamble, T. R., Murphy, E. C., de Vos, A. M., & Schultz, P. G. (1993) *Science 261*, 1578.
Libson, A. M., Gittis, A. G., & Lattman, E. E. (1994) *Abstr. ASBMB Mtg* (Washington D.C.) *FASEB J. 8*, A1278.
Loll, P. J., & Lattman, E. E. (1989) *Proteins 5*, 183.
Loll, P. J., & Lattman, E. E. (1990) *Biochemistry 29*, 6866.
Luzzati, P. V. (1952) *Acta Crystallogr. 5*, 802.
Mehdi, S., & Gerlt, J. A. (1982) *J. Am. Chem. Soc. 104*, 3223.
Poole, L. B., Lovey, D. A., Hale, S. P., Gerlt, J. A., Stanczyk, S. M., & Bolton, P. H. (1991) *Biochemistry 30*, 3621.
Pourmotabbed, T., Dell'Acqua, M., Gerlt, J. A., Stanczyk, S. M., & Bolton, P. H. (1991) *Biochemistry 29*, 3677.
Sack, J. S. (1988) *J. Mol. Graphics 6*, 224.
Serpersu, E. H., Shortle, D., & Mildvan, A. S. (1986) *Biochemistry 25*, 68.
Serpersu, E. H., Shortle, D., & Mildvan, A. S. (1987) *Biochemistry 26*, 1289.
Serpersu, E. H., McCracken, Peisach, J., & Mildvan, A. S. (1988) *Biochemistry 27*, 8034.
Shortle, D., & Lin, B. (1985) *Genetics 110*, 539.
Torchia, D. A., Sparks, S. W., & Bax, A. (1989) *Biochemistry 28*, 5509.
Tucker, P. W., Hazen, E. E., & Cotton, F. A. (1978) *Mol. Cell. Biochem. 22*, 67.
Wang J., Le Master, D. M., & Markley, J. L. (1990) *Biochemistry 29*, 88.
Weber, D. J., Serpersu, E. H., Shortle, D., & Mildvan, A. S. (1990) *Biochemistry 29*, 8632.
Weber, D. J., Gittis, A. G., Mullen, G. P., Abeygunawardana, C., Lattman, E. E., & Mildvan, A. S. (1992) *Proteins 13*, 275.
Weber, D. J., Serpersu, E. H., Gittis, A. G., Lattman, E. E., & Mildvan, A. S. (1993) *Proteins 17*, 20.
Weber D. J., Libson, A. M., Gittis, A. G., Lebowitz, M. S., & Mildvan, A. S. (1994) *Biochemistry 33* (following paper in this issue).
Yamashita, M. M., Almassy, R. J., Janson, C. A., Cascio, D., & Eisenberg, D. (1989) *J. Biol. Chem. 264*, 17681.